Pseudopotential study of binding properties of solids within generalized gradient approximations: The role of core-valence exchange-correlation.

M. Fuchs, M. Bockstedte,* E. Pehlke,† and M. Scheffler
Fritz-Haber-Institut der Max-Planck-Gesellschaft, Faradayweg 4-6, D-14195 Berlin-Dahlem, Germany
(submitted to Phys. Rev. B, July, 11, 1997)

In *ab initio* pseudopotential calculations within density-functional theory the nonlinear exchange-correlation interaction between valence and core electrons is often treated linearly through the pseudopotential. We discuss the accuracy and limitations of this approximation regarding a comparison of the local density approximation (LDA) and generalized gradient approximations (GGA), which we find to describe core-valence exchange-correlation markedly different. (1) Evaluating the binding properties of a number of typical solids we demonstrate that the pseudopotential approach and namely the linearization of core-valence exchange-correlation are both accurate and limited in the same way in GGA as in LDA. (2) Examining the practice to carry out GGA calculations using pseudopotentials derived within LDA we show that the ensuing results differ significantly from those obtained using pseudopotentials derived within GGA. As principal source of these differences we identify the distinct behavior of core-valence exchange-correlation in LDA and GGA which, accordingly, contributes substantially to the GGA induced changes of calculated binding properties.

PACS numbers: 71.15.Mb, 71.15.Hx, 71.15.Nc, 61.50.Lt

I. INTRODUCTION

Generalized gradient approximations (GGAs) to the exchange-correlation (XC) energy[1–5] in density-functional theory[6,7] are currently receiving growing interest as a simple alternative to improve over the local density approximation (LDA)[8,9] in *ab initio* total energy calculations. In various respects the GGA proved to be more appropriate than the LDA, namely (1) Binding energies of molecules[10,11] and solids[12–14] turn out more accurate, correcting the tendency of the LDA to overbinding. (2) Activation energy barriers, e.g. for the dissociative adsorption of H_2 on metal and semiconductor surfaces[15–17] are in distinctly better accordance with experiment. Reaction and activation energies for a variety of chemical reactions show a similar improvement.[18–20] (3) The relative stability of structural phases seems to be predicted more realistically for magnetic[21] as well as for nonmagnetic[22,23] materials. Bulk structural properties are often not improved within GGA. While the lattice parameters consistently increase compared to the LDA, a closer agreement with experimental data is reported for alkali, $3d$, and some $4d$ metals.[5,24–26] An overestimation of up to several percent is found however for $5d$ metals and common semiconductors, their bulk modulus turning out too small accordingly (typically by $\lesssim 25\%$).[27–29]

Regarding the understanding of the GGA and further advances beyond it, it is important to gain insight into the XC related "mechanisms" underlying an eventually improved performance, e.g. along the lines pursued in Refs. 5,12,30, and 31. Complementary, careful estimates are needed to what degree computational approximations in evaluating the total energy interfere with a comparison of different XC functionals. With this in mind we examine two interrelated issues that have been of persistent concern in comparison of the LDA and the GGA based on pseudopotential calculations.[32]

Firstly in how far the nonlinearities associated with the XC interaction of core and valence electrons in these XC density-functionals can be accounted for by the pseudopotentials. Computationally it is expedient to treat core-valence XC as a part of the pseudopotential and thus as if it acted linearly on the (pseudo) valence electron density. Within the LDA the transferability of the pseudopotentials remains, in most cases, intact under this approximation, i.e. good agreement of the results of pseudopotential with all-electron calculations may be expected without handling these nonlinearities explicitly. The extent to which this carries over to GGA's, and thus enables a menaningful comparison with the LDA, is unclear at present. Experience with GGA's still needs to be built up and previous studies have advanced conflicting views on this subject: Examining structural parameters of crystalline solids, Juan *et al.*[33,34] concluded nonlinear core corrections for XC were required in pseudopotential calculations within the GGA by Perdew and Wang[5] (PW) even in cases where they are negligible in LDA, like bulk Si. On the other hand, Moll *et al.*[23] and Dal Corso *et al.*[27] found the LDA and PW GGA behaved alike in this respect.

Secondly we discuss the role of differences seen in the pseudopotentials constructed within the LDA and within the GGA. Here we address, on the one hand, in how far such differences are small enough to warrant the circumventing of a full self-consistent GGA calculation (using GGA pseudopotentials) by a computationally simpler *post*-LDA treatment where the electronic total energy is first minimized within LDA (using LDA pseudopotentials) and then corrected perturbatively for the GGA XC energy. On the other hand, the behavior of the pseudopotentials eventually reflects a different description of the core-valence interactions in LDA and GGA. This allows us to conceive the GGA-related effects separately in terms of XC among the valence electrons themselves and XC of the valence with the core electrons. Results in several works indeed hint that the LDA and GGA might differ in this respect: Garcia *et al.*[14] evaluated cohesive properties of some metals and semiconductors on the ba-

sis of the Becke/Perdew (BP) GGA[3,4] and a precursor to the PW GGA. Dependent on whether the pseudopotentials screened within the GGA were derived from an LDA or GGA calculation of the free atom they obtained, in some instances, differing values of the lattice parameters *and* cohesive energies. Examining the dissociation of silanes using LDA-based pseudopotentials Nachtigall *et al.*[35] observed noticeably overestimated activation and reaction energies compared to the respective all-electron approach for various GGAs, but close agreement for the LDA. Despite the apparent incongruencies, GGA calculations are still being based on LDA pseudopotentials.[36,37]

To address these issues we investigate the differences between the LDA and GGA systematically at each step of the pseudopotential approach, the construction of the pseudopotentials from atomic calculations and their use in polyatomic systems. In turn we evaluate the cohesive properties of a set of typical metallic, semiconducting, and insulating crystals (Na, Mg, Al, Cu, W, diamond, Si, Ge, GaAs, and NaCl), where we apply pseudopotentials with and without nonlinear core corrections. With respect to the role of core-valence XC we establish in how far its handling affects the accuracy of pseudopotential calculations by comparing our results with available all-electron data. We then discuss the related need for the consistent use of the same XC scheme at all points of a pseudopotential calculation and comment on the contribution to the GGA induced changes of LDA results for cohesive properties driven by differences between LDA and GGA core-valence XC.

Concerning proposals for GGAs we present results for the PW and the earlier BP schemes. Both are variants of the generic type

$$E_{\rm XC}^{\rm GGA}[n] = \int n(\mathbf{r})\epsilon_{\rm XC}^{\rm GGA}(n(\mathbf{r}),\nabla n(\mathbf{r}))\,d^3r, \qquad (1)$$

depending locally on the electronic density $n(\mathbf{r})$ and its gradient and yielding a local XC potential $V_{\rm XC}(\mathbf{r}) = \delta E_{\rm XC}[n]/\delta n(\mathbf{r})$ like in case of the LDA. These schemes are widely used in present day applications, and remain of interest as a starting point in recent nonlocal hybrid XC schemes expected to further improve over GGA type functionals.[38] Accurate all-electron results are available for those GGA schemes and serve as a rigorous reference for the pseudopotential calculations in this study. The PW GGA is derived basically from first principles, combining the gradient expansions of the exchange and correlation holes of a non-uniform electron gas with real-space truncations to enforce constraints imposed by properties of the physical XC hole. While the BP GGA may be deemed to be somewhat more heuristic as it relies also on fitted parameters, it has been yielding results close to those of the PW GGA, at least in all-electron calculations. In addition we have considered the recently proposed GGA by Perdew, Burke and Ernzerhof (PBE) which is regarded to be conceptually more concise than the PW GGA but is expected to perform essentially similarly.[39] In the pseudopotential calculations for the properties addressed here we have found the PBE and the PW GGA to yield nearly equivalent results,[40] hence our conclusions for the PW GGA hold for the PBE GGA as well.

The remainder of this paper is organized as follows: In Sec. II we briefly review and discuss the relevant formal aspects of pseudopotential calculations. Technical characteristics of our calculations are outlined in Sec. III. In Sec. IV we report our results, and put them in perspective with our considerations from Sec. II. Section V summarizes our conlcusions. Atomic units are used throughout unless indicated otherwise.

II. GENERAL CONSIDERATIONS

In pseudopotential calculations the total energy is formally treated as a functional of the valence charge density alone, with the pseudopotentials accounting for the interaction of the valence electrons with the nuclei and with the core electrons - namely for Pauli repulsion, electrostatic and XC interactions - to within the frozen core approximation.[41,42] Substituting the GGA for the LDA modifies the treatment not only of the XC interactions of the valence electrons among themselves but also that of the core-valence (CV) interactions. In order to treat all interactions within one and the same XC scheme the pseudopotentials to be employed in a GGA calculation in principle ought to be generated *consistently* within the same GGA as well, rather than within, say, the LDA. In the following we discuss the relevance of this "pseudopotential consistency" to total energy calculations in LDA and GGA. Within the pseudopotential framework the GGA total energy functional reads

$$E_{\rm tot}^{\rm GGA}[n] = T_0[n] + E_{\rm H}[n] + E_{\rm XC}^{\rm GGA}[n] + \sum_i^{\rm occ}\langle\psi_i|\hat{V}^{\rm GGA}|\psi_i\rangle, \qquad (2)$$

where the various terms denote the noninteracting kinetic energy, the Hartree energy, the XC energy and the potential energy of the valence electrons, represented by the pseudo wavefunctions $\psi_i(\mathbf{r})$ and the corresponding charge density $n(\mathbf{r}) = \sum_i^{\rm occ}|\psi_i(\mathbf{r})|^2$ in the presence of the ion cores, represented by GGA pseudopotentials, $\hat{V}^{\rm GGA}$. The LDA counterpart to (2) is obtained by substituting the XC energy $E_{\rm XC}^{\rm LDA}$ and the LDA pseudopotentials $\hat{V}^{\rm LDA}$ for the respective GGA entities.

Now the groundstate energies in GGA and LDA can be readily compared with the help of a perturbative analysis of the total energy functionals $E_{\rm tot}^{\rm GGA}[n]$ and $E_{\rm tot}^{\rm LDA}[n]$, at any given set of ionic positions. Around the respective stationary groundstates, characterized by the densities $n^{\rm GGA}$ and $n^{\rm LDA}$, the variational principle implies that

$$E_{\rm tot}^{\rm GGA}[n] \simeq E_{\rm tot}^{\rm GGA}[n^{\rm GGA}] + \mathcal{O}[(n-n^{\rm GGA})^2], \qquad (3)$$

and likewise in LDA. Supposed GGA and LDA yield similar densities the difference of their groundstate energies, $\delta E_{\rm tot} = E_{\rm tot}^{\rm GGA}[n^{\rm GGA}] - E_{\rm tot}^{\rm LDA}[n^{\rm LDA}]$, can be expressed by virtue of (3) as

$$\begin{aligned}\delta E_{\rm tot} \simeq\ & E_{\rm XC}^{\rm GGA}[n^{\rm LDA}] - E_{\rm XC}^{\rm LDA}[n^{\rm LDA}] \\ & + \sum_i^{\rm occ}\langle\psi_i^{\rm LDA}|\hat{V}^{\rm GGA} - \hat{V}^{\rm LDA}|\psi_i^{\rm LDA}\rangle,\end{aligned} \qquad (4)$$

i.e. simply in terms of the density and wavefunctions obtained within the LDA, using the LDA pseudopotential, $\hat{V}^{\rm LDA}$. Accordingly the GGA modifies the (pseudo) total energy in two ways: (i) By the direct difference of the XC energies $\delta E_{\rm XC} = E_{\rm XC}^{\rm GGA}[n^{\rm LDA}] - E_{\rm XC}^{\rm LDA}[n^{\rm LDA}]$. This term corresponds to the often applied *a posteriori* gradient-correction scheme where, at given ionic coordinates, the density is evaluated self-consistently from the LDA XC potential and then used to compute the total energy with the GGA XC energy functional. For the GGAs considered the $\delta E_{\rm XC}$ is negative, and vanishes in the limiting case of the homogeneous electron gas. Typically its magnitude increases with the degree of inhomogeneity of the system at hand,[23] the GGA correction to the LDA XC energy being larger for a free atom or molecule than in a solid. (ii) By the potential energy correction, $\delta E_V = \sum_i^{\rm occ} \langle \psi_i^{\rm LDA} | \hat{V}^{\rm GGA} - \hat{V}^{\rm LDA} | \psi_i^{\rm LDA} \rangle$, which arises as a consequence of the pseudopotential approximation and eventually reflects the differences in the behavior of the CV interactions in LDA and GGA. Note that in an all-electron formulation this term would be absent altogether. Clearly the potential energy correction is missed when LDA pseudopotentials are carried over to GGA calculations, giving rise to a "portability" error compared to the consistent GGA calculation using GGA pseudopotentials. We shall demonstrate in Section IV that δE_V does not cancel out when total energy differences are considered but is in general of similar importance as $\delta E_{\rm XC}$ for quantitative tests of the GGA within the pseudopotential framework.

For an understanding of the differences between the GGA and LDA it is worthwile to examine more closely the various contributions to the CV interactions the pseudopotentials mediate. In the following we identify and discuss these for norm-conserving pseudopotentials,[43] constructed by standard schemes[44,45] from atomic all-electron calculations. As a canonical first step these algorithms generate angular momentum dependent screened pseudopotentials $V_l^{\rm eff}[n_0]$ from a particular reference configuration, e.g. the groundstate of the neutral atom, assuming spherical screening. These act as effective potentials on the atomic pseudo valence states via the radial Schrödinger equations,

$$\left(-\frac{1}{2}\frac{d^2}{dr^2} + \frac{l(l+1)}{2r^2} + V_l^{\rm eff}[n_0;r] - \varepsilon_l\right) r R_l(r) = 0. \quad (5)$$

The $V_l^{\rm eff}[n_0]$ contain a common spherical screening potential which is self-consistent with the *total* atomic charge density $n_0(r)$, comprised of the (pseudo) valence density n_0^v and the core charge density n_0^c obtained from the all-electron core states. The effective potentials can be decomposed rigorously into the Hartree potentials $V_{\rm H}$ and the XC potential due to the valence and core electrons and an angular momentum dependent bare potential $V_l^{\rm bare}$ which conveys the nuclear attraction and the Pauli repulsion due to the core states; for an arbitrary valence configuration one has

$$\begin{aligned} V_l^{\rm eff}[n;r] = V_l^{\rm bare}(r) &+ V_{\rm H}[n_0^c;r] \\ &+ V_{\rm H}[n^v;r] + V_{\rm XC}[n^v + n_0^c;r], \end{aligned} \quad (6)$$

which, in the reference configuration ($n = n_0^v + n_0^c$), reduces of course to the screened pseudopotentials. Through the nonlinearity of the XC potential in the density the effective potential retains a dependence on the total rather than on the valence density alone as it is ultimately a prerequisite for an efficient plane wave representation. Customarily a further separation in terms of frozen core and variable valence contributions is accomplished by "linearizing" the XC interaction taking

$$\begin{aligned} V_{\rm XC}[n^v + n_0^c;r] \simeq\ & V_{\rm XC}[n^v + \tilde{n}_0^c;r] \\ &+ \left(V_{\rm XC}[n_0^v + n_0^c;r] - V_{\rm XC}[n_0^v + \tilde{n}_0^c;r]\right), \end{aligned} \quad (7)$$

where the partial core density $\tilde{n}_0^c(r)$ serves as a control parameter. Choosing $n^v = n_0^v$ the screened pseudopotentials, and thus the atomic properties in the reference configuration, are correctly recovered. Now those terms on the RHS of (6) which are independent of the valence density define the usual pseudopotentials that are to be transferred to and screened according to the environment of one's target system. Applying (7) they read

$$\begin{aligned} V_l(r) = V_l^{\rm bare}(r) &+ V_{\rm H}[n_0^c;r] \\ &+ \left(V_{\rm XC}[n_0^v + n_0^c;r] - V_{\rm XC}[n_0^v + \tilde{n}_0^c;r]\right). \end{aligned} \quad (8)$$

The last term here comprises the core-valence XC interaction

$$\Delta V_{\rm XC}(r) = \left(V_{\rm XC}[n_0^v + n_0^c;r] - V_{\rm XC}[n_0^v + \tilde{n}_0^c;r]\right) \quad (9)$$

as represented by the ionic pseudopotential. Below we demonstrate that it is the key quantity to understand the differences between the ionic pseudopotentials in LDA and GGA which, in practice, are defined simply by "unscreening" the screened potentials according to

$$V_l(r) = V^{\rm eff}[n_0;r] - V_{\rm H}[n_0^v;r] - V_{\rm XC}[n_0^v + \tilde{n}_0^c;r]. \quad (10)$$

with all quantities evaluated within the respective XC scheme. Note that the transformation Eq. (7) turns the core-valence XC energy into a linear functional of the valence density that is absorbed in the pseudopotential contribution to the total energy instead of being treated as a part of the XC energy itself. By experience the complete core-valence linearization, $\tilde{n}_0^c(r) = 0$, has proven to be accurate for the majority of applications within the LDA. It is expected to be justified for local functionals like the LDA and also the GGA if the overlap of the core and valence charge densities does not substantially change whenever chemical bonds are formed or altered. Formally the nonlinear core-valence XC could be regarded exactly, taking $\tilde{n}_0^c(r) = n_0^c(r)$, and, correspondingly, $E_{\rm XC} =: E_{\rm XC}[n + \tilde{n}_0^c]$ in the total energy functional (2), where $\tilde{n}_0^c$ denotes the core charge density as compounded from the frozen atomic core charge densities. Since the core states are strongly localized and sharply peaked such a choice is beyond the realm of a plane wave representation however. If a complete linearization of CV XC proves insufficient, e.g. in calculations of alkali metals[46] or involving spin-polarization,[24] the nonlinearities can still be captured adequately in the chemically most important interatomic regions with the help of a partial core density, as was first realized by Louie *et al.*[47] It is

tailored to coincide with the full core charge density beyond a suitable cutoff radius r_c but avoids the sharply peaked structure close to the nucleus by a smooth cutoff function $b(r)$ chosen largely at computational expediency, *cf.* Ref. 47 and Sec. IV,

$$\tilde{n}_0^c(r) = \begin{cases} n_0^c(r) & \text{for } r \geq r_c, \\ b(r) n_0^c(r) & \text{for } r < r_c, \text{ with } b(r) \leq 1. \end{cases} \quad (11)$$

Note that the CV XC component of the ionic pseudopotentials vanishes beyond r_c.

It is well understood that the GGA does not substantially alter the wavefunctions and the spectrum of atomic valence states compared to the LDA, these are bound too weakly in both schemes,[30] mainly because the XC potentials of these schemes insufficiently cancel the repulsive contribution from the electrons' self-interaction to the Hartree potential. Consequently the effective potentials (6) for the pseudo valence states ought to be close for both XC schemes. Indeed the screened LDA and GGA pseudopotentials are barely distinguishable by a simple visual inspection as can be seen, e.g., for germanium and copper in Fig. 1.

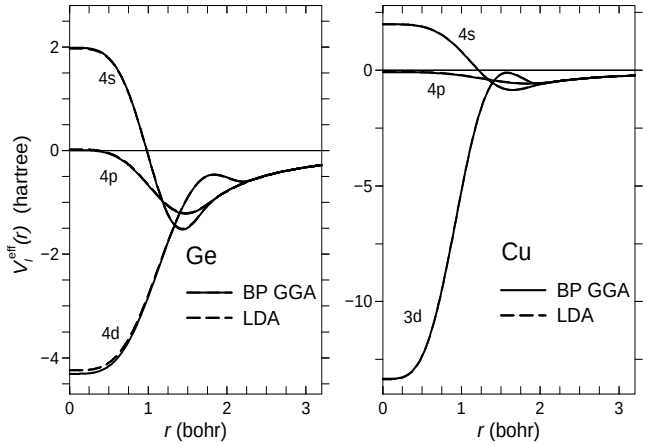

FIG. 1. Screened pseudopotentials within BP GGA and LDA for germanium and copper. On the scale of these plots the GGA and LDA pseudopotentials lie one on top of each other. Shown are Troullier-Martins pseudopotentials with cutoff radii $r_{s,p} = 1.9$ bohr and $r_d = 2.3$ bohr (Ge), and $r_{s,d} = 2.0$ bohr and $r_p = 2.3$ bohr (Cu).

Turning to the unscreened, ionic pseudopotentials actually used for calculations more pronounced deviations between LDA and GGA pseudopotentials emerge. These may by easily analyzed in terms of the various pseudopotential components given by Eqs. (8) and (7) which contribute to the difference $\delta V_l(r) = V_l^{\rm GGA}(r) - V_l^{\rm LDA}(r)$, where the superscripts indicate the type of XC employed in constructing the pseudopotentials. This decomposition is illustrated in Fig. 2, weighting all differences with the r-dependent volume element. To highlight the role of the individual contributions we distinguish three cases:

(i) completely linearized XC, $\tilde{n}_0^c(r) = 0$.

(ii) approximate account of nonlinear CV XC, employing a partial core charge density identical with the full one outside $r_c = 1.3$ bohr.

(iii) full account of nonlinear CV XC, taking $\tilde{n}_0^c(r) = n_0^c(r)$.

Case (iii) serves to identify the *genuine* difference potential, due to the unlike bare and core-valence Hartree potentials. These originate just from the small differences of the self-consistent atomic orbitals in LDA and GGA and thus remain the same in (i) and (ii) where CV XC is approximated. The core-valence Hartree potentials are seen to make a small positive contribution,

$$\delta V_{\rm H}(r) = V_{\rm H}[n_0^c({\rm GGA}); r] - V_{\rm H}[n_0^c({\rm LDA}); r].$$

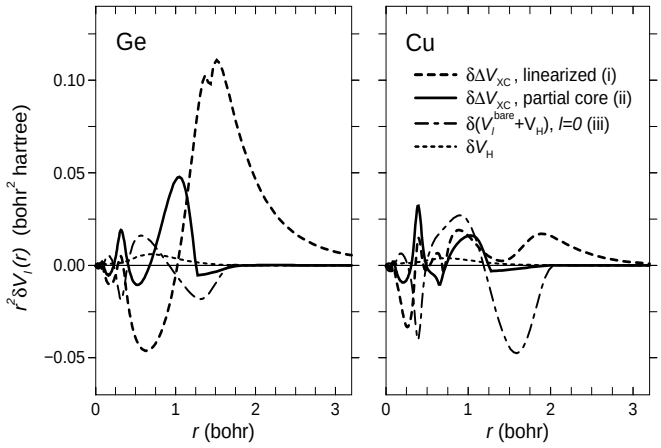

FIG. 2. Difference of the ionic pseudopotentials in BP GGA and LDA for germanium and copper, corresponding to the screened potentials given in Fig. 1. Shown are the XC, Hartree, and bare potential contributions, *cf.* Eq. (8), as discussed in the text. Both panels use the same scale for the ordinate. The cutoff radius of the partial core charge densities was chosen as 1.3 bohr.

This reflects the fact that the core states are more tightly bound in GGA than in LDA, somewhat enhancing the electrostatic screening of the nuclei.[48,30] Still $\delta V_{\rm H}$ is found to be weaker and faster decaying than the (oscillatory) differences in the bare potentials. In case (i) the *genuine* difference potential is superimposed with a long ranged, repulsive hump. This feature clearly signifies the distinct analytical behavior of the CV XC potentials, Eq. (9), in LDA and GGA, rather than differences in the self-consistent charge densities. Notably for germanium it attains its maximum around and stretches well beyond the maximum of the valence charge density up to radii that correspond to mid-bond positions. Including a partial core charge density, case (ii), eliminates by construction the core-valence XC potentials outside the respective cutoff radius in both LDA and GGA. In this region one therefore recovers the more short ranged, and in case of germanium weaker, genuine difference potential. Inside there remains some interference of genuine and core-valence XC related differences as partial and full core charge density deviate from each other.

The above discussion suggests that the distinct core-valence XC interaction in LDA and GGA is a prime

source of the differences between the pseudopotentials. As the LDA pseudopotentials and their GGA counterparts differ even in interatomic regions they are to be expected to perform unlike in a pseudopotential calculation which employs the GGA for the XC energy, germanium with linearized CV XC being a generic example. By explicitly considering nonlinear CV XC, or, as exemplified by copper, by including more semicore states as valence states the difference in CV XC is removed from the pseudopotentials and instead taken into account through the XC energy functionals themselves. In this case LDA and GGA pseudopotentials should thus behave more alike, provided of course the cooperative genuine differences are negligibly small themselves. In Sec. IV we substantiate these aspects quantitatively.

III. COMPUTATIONAL METHOD

From a practitioner's point of view, GGAs are readily incorporated in plane wave based schemes: the derivatives of the density needed to compute XC energy and potential in position space are evaluated from the reciprocal space representation of the density and transformed to position space using Fourier transformations, the convergence of all relevant quantities being controlled - like in case of LDA - through the plane wave basis size. The construction of norm-conserving pseudopotentials within GGA's proceeds entirely parallel to the one in LDA. The necessary radial density gradients may be inferred, e.g., directly from the derivatives of the radial wavefunctions.

We have constructed the pseudopotentials[49] based on a scalar-relativistic atomic calculation using the scheme of Troullier and Martins.[44] Core and valence states were partitioned as usual, i.e. retaining only the uppermost occupied s and p states as valences, except for Cu and W where the $3d\,(5d)$ states need to be included in the valence space. The resulting semilocal potentials were further transformed into fully separable representations of the Kleinman-Bylander kind.[50] In case of nonlinear CV XC we used a cuspless polynomial to represent the partial core charge density inside the cutoff radius. Continuity of the density up to its third derivative is enforced to ensure that the GGA XC potential joins smoothly. Various tests, carried out for the free pseudo atoms and described in the appendix, indicate comparable transferability for the GGA and LDA pseudopotentials. The ionic pseudopotentials are tabulated and transferred without any intermediate fitting to the plane wave calculation. We have refrained from any smoothing[33] of the ionic GGA pseudopotentials which on occasion display short-ranged oscillations, mostly for the PW GGA.[29,39] These correspond to a plane wave energy regime where the kinetic energy is dominating all other energy contributions and may, therefore, be conceived to be physically negligible. Care is required though to leave the relevant low Fourier components intact if smoothing is performed. With a numerical tabulation this is attained in an unbiased, systematic manner through the basis size cutoff.

We have computed[51] the total energy per atom in the bulk systems varying the lattice constant within about $\pm 5\%$ of the respective equilibrium value. Fitting these energies to Murnaghan's equation of state[52] we obtained the equilibrium values of the lattice parameters and the total energy per atom. The cohesive energy was determined by subtracting the latter from the total energy of the spin-saturated spherical (pseudo) atom. To correct this value for neglected contributions due to the spin-polarization of the atomic groundstate, we added the difference of the total energies of the spin-polarized and spin-saturated all-electron atom within the respective XC scheme. Corrections of the theoretical values of the cohesive energy for the phonon zero-point energies are disregarded, they amount to $\approx$180 meV for diamond and are expected to stay below $\approx$60 meV for the other solids.[53] The Brillouin zone sampling for the bulk systems was carried out using $6 \times 6 \times 6$ (diamond, NaCl), $8 \times 8 \times 8$ (Al, Si, Ge, GaAs), and $10 \times 10 \times 10$ (Na, Cu, W) meshes of special $\mathbf{k}$-points.[54] For evaluating the cohesive energies we chose a plane wave cutoff energy of 50 Ry for all crystals other than diamond, Cu, and W for which we used 100 Ry. The respective structural parameters were determined with roughly two thirds of these values. These computational parameters allow for a numerical precision of better than 0.5% for the lattice constants and better than 50 meV for the binding energies.[55]

IV. RESULTS AND DISCUSSION

Two sets of GGA calculations were performed where we adopted either the consistent GGA approach, employing the GGA for both plane wave calculation *and* construction of the the pseudopotentials, or, by contrast, the inconsistent GGA approach, employing the GGA for the plane wave calculation but LDA for the construction of the the pseudopotentials. The results of our calculations are compiled along with reference data in the Tables IV - VIII. By a comparison with all-electron data and calculations including nonlinear CV XC we first demonstrate the pseudopotentials to be as transferable within the GGA as in the LDA. In particular transferability is not more stringently limited by nonlinear CV XC in GGA than in LDA. This provides the frame of reference for our subsequent examination of the consistent and inconsistent GGA approaches which are found to be inequivalent indeed. Following our discussion of Sec. II we then show that the perturbative potential energy correction yields a good quantitative account of the differences between these approaches. Together with the fact that the discrepancies are essentially eliminated once nonlinear CV XC is included, this allows us to identify these discrepancies as a manifestation of the distinct behavior of CV XC in LDA and GGA. Namely we find CV XC to contribute significantly to the correction of the binding energies and lattice parameters induced by the GGA.

A. Pseudopotential transferability within GGA

Possible uncertainties rooted in the pseudopotential approximation itself are properly distinguished from ef-

fects due to the use of different XC functionals by a comparison with all-electron data. To this extent we show in Fig. 3 the relative error of the lattice constant with respect to its experimental value based on a compilation of results from recent all-electron calculations[25,28] and as obtained in the present pseudopotential framework, accounting for nonlinear CV XC and working with the consistent approach to PW GGA. It can be seen that in LDA as well as in PW GGA the results of the pseudopotential and the all-electron method agree on the order of or better than 1%. In particular both methods yield virtually the same lattice expansion due to the GGA compared to LDA. Merely in case of Al the agreement is not fully quantitative. Concerning the bulk moduli we note that the pseudopotential calculations reproduce the reduction of the LDA values due to the GGA as obtained from the all-electron calculations. The residual discrepancies between pseudopotential and all-electron results for the bulk moduli of Ge and GaAs in LDA as well as in GGA may be seen as a reminder that a more accurate treatment requires the extended $3d$ states of Ga and Ge to be considered as valence states.[28]

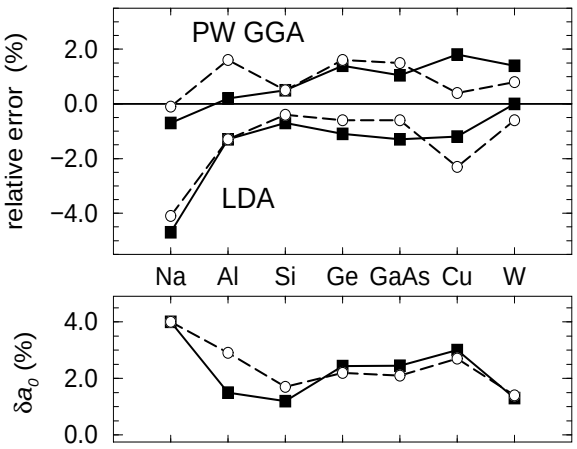

FIG. 3. Top panel: Relative error of the bulk lattice constant evaluated within LDA and GGA with respect to the experimental value. Filled squares refer to the present work, open circles to all-electron results of Refs. 25 and 28. Bottom panel: Increase of the bulk lattice constant (δa_0) from the LDA to the GGA value relative to the experimental value for either method.

The routine disregard of nonlinear CV XC entails no alterations of the calculated lattice properties compared to the results obtained with explicit account of nonlinear CV XC for diamond, Al, and Si. For Ge and GaAs the lattice constants are reduced by ≈1% in LDA and changed somewhat less in GGA. The values of the lattice constants of sodium metal turn out smaller by ≈2% in LDA and change again less for the GGAs. Those of NaCl agree with the experimental values at the usual level, but turn out unrealistic with linear CV XC. It is well established that an explicit account of nonlinear CV XC is essential in order to predict dependable lattice properties for compounds of alkali metals within the LDA.[46] Our results for NaCl suggest that this conclusion applies to the GGAs as well. Such a behavior seems reasonable, as in view of the relatively easily polarizable valence shell of Na its core-valence overlap in metallic sodium or NaCl is likely to depart considerably from the one in the isolated Na atom so that an explicit account of the ensuing nonlinear changes of core-valence XC becomes indispensable at large. The presence of slight differences in the calculated lattice properties with and without explicit nonlinear CV XC for GaAs, Ge, and W can be similarly conceived as a signature of the extended core charge densities in these atoms compared to C, Al and Si, for which such differences are not observed. They are likewise absent in copper, where the semicore $3d$-electrons are considered as valence states so that their XC interactions with the $4s$-electrons are incorporated exactly. Thus we altogether find the neglect of nonlinear CV XC within the GGAs of similar importance to the transferability of the pseudopotentials as within LDA. In all cases where nonlinear CV XC is dispensable in LDA it proved to be negligible in the GGAs as well. Judged by the systems and properties considered we clearly find the pseudopotential approach itself to be equally applicable and accurate in GGA as in LDA.

Our results compare well with those of previous pseudopotential calculations reported in Refs. 14 (BP GGA) and 27 (BP and PW GGA), and Ref. 34 (PW GGA). The severe overcorrection of the lattice constants of Al, Si, Ge, and GaAs in case of PW GGA without nonlinear CV XC found by Juan and Kaxiras[33] is not confirmed here. Similar to Ref. 27 our findings do namely not support the conjecture put forward by these authors in Ref. 34 that an explicit treatment of nonlinear CV XC were necessary in order to arrive at transferable pseudopotentials within the PW GGA.

For the present sytems we find both GGAs to predict closely agreeing structural properties with only immaterial differences. Compared to the LDA we note enhanced agreement with experimental data regarding the lattice constants of Na, Mg, Al, and Si. For the other materials the GGA functionals overestimate the lattice constants to a similar degree as LDA underestimates them. The bulk moduli within the GGAs are predicted in good accordance with experiment only for Na and Cu, for the other materials they are clearly underestimated, in particular (by up to ≈ 25%) for the semiconductors. In all cases the PW GGA yields cohesive energies in close agreement with experimental figures and corrects the overbinding of the LDA. Observe however that in GGA the values of the atomic energy and hence the cohesive energy were still lowered by up to several tenth of an eV by allowing for nonspherical groundstate densities,[12,56] possibly unveilling a slight "underbinding" indicated already by the overestimate of the lattice parameters. We note the BP GGA to yield cohesive energies systematically lower than in the PW GGA suggesting a slightly weaker binding than the PW GGA.

B. LDA vs. GGA pseudopotentials in GGA calculations

Having reassured ourselves of the validity of the pseudopotential ansatz itself we now turn to an account of

the inconsistent GGA approach where LDA rather than GGA pseudopotentials are employed. As argued in Section II, LDA and GGA pseudopotentials exhibit substantial differences even in the interatomic regions of molecular or crystalline compounds. This eventually implies that LDA and GGA pseudopotentials perform differently when they are combined with the GGA XC energy functionals.

It is evident from the results listed in Tables I - VIII that the outcome of the inconsistent approach depends sensitively on the handling of core-valence XC. We shall address linear CV XC first. Within it, the inconsistent GGA approach yields a description of the cohesive properties clearly disparate to that obtained from the consistent one: the characteristic lattice expansion in either BP or PW GGA does not occur, and instead the lattice parameters closely resemble their LDA values. Likewise the cohesive energies turn out larger by 0.3 eV to 0.7 eV, amounting to ≈10% (diamond) up to ≈50% (Ge) of the GGA correction to the cohesive energy found with GGA PPs. A somewhat modified behavior is observed for copper where the lattice parameters are close to those from the consistent GGA approach and the cohesive energy correction turns out larger by about 0.2 eV than with GGA pseudopotentials. We find the consistent and the inconsistent GGA approach to both yield congruous descriptions of the binding properties once the calculations include nonlinear CV XC: the inconsistent GGA approach uniformly recovers the typical lattice expansion as well as the decrease of the cohesive energy. The only incongruencies found between the two approaches concern residual deviations of about 0.2 eV for the cohesive energies of diamond and copper.

To further discuss the GGA correction of the cohesive energy, δE_b, dependent on the choices for pseudopotential and the treatment of CV XC, we examine the constituent corrections of the total energies for (pseudo) atom and solid separately by the decomposition

$$\begin{aligned} \delta E_b &\equiv E_b^{\mathrm{GGA}} - E_b^{\mathrm{LDA}} \\ &= \delta E_{\mathrm{tot}}^{\mathrm{atom}} - \delta E_{\mathrm{tot}}^{\mathrm{solid}}, \end{aligned} \tag{12}$$

making use of the the perturbative analysis of Section II. Following Eq. (4) the GGA entails a twofold change of the total energy compared to the LDA: the direct correction of the XC energy, δE_{XC}, and the potential energy correction, δE_{V}. Now the consistent approach comprises both corrections so that the change in total energy is given by $\delta E_{\mathrm{tot}} \simeq \delta E_{\mathrm{XC}} + \delta E_{\mathrm{V}}$. By contrast the inconsistent approach neglects the difference of the LDA and GGA pseudopotentials so that δE_{V} vanishes and the change in total energy is limited to $\delta E_{\mathrm{tot}} \simeq \delta E_{\mathrm{XC}}$. In Table XI we detail the various terms for some exemplary cases.

We first of all see the perturbative treatment to be well justified as it closely reproduces the total energy corrections extracted from the respective self-consistent LDA and GGA calculations in both the atoms and the solids to within 0.02 eV. Adopting *linear* CV XC, the XC energy correction in each case is found to account only partly for the GGA induced change of the cohesive energy. Instead a substantial fraction must be attributed to the potential energy correction and is thus indeed effected by the difference of the LDA and GGA pseudopotentials. Acting in a like manner as δE_{XC}, δE_{V} results in a decrease of the cohesive energy, except for copper where we observe the above mentioned slight enlargement. Taking nonlinear CV XC into consideration, the magnitude of the potential energy correction is reduced compared to linear CV XC. Importantly, δE_{V} no longer contributes to the change of the binding energy which is instead captured completely by the XC energy correction for Na, Si and Ge, shown in detail in Table XI. It does retain significance in case of diamond and copper however. Save for these, the inconsistent and consistent approaches with explicit nonlinear CV XC thus produce alike values for the binding energies.

We note the lattice expansion observed upon switching over from LDA to GGA to be consistent with the repulsive character of the difference potential between the LDA and GGA pseudopotentials seen in the real space inspection of the respective pseudopotentials, *cf.* Fig. 2. Similarly the potential energy correction turns out positive, and more so in the solid where valence charge accumulates in the bonding region. Once nonlinear CV XC is taken into account, the XC related differences outside the core region are eliminated. What remains are essentially the genuine differences of the LDA and GGA pseudopotentials, reflecting the different description of the core states in the respective XC schemes. In principle the more tightly bound core states in the GGA should make the Pauli and the Coulomb repulsion more short-ranged compared to the LDA, adding some repulsion about the ion sites and some attraction at intermediate distances. The details are certainly quite species dependent and moreover one cannot rule out some interference from residual XC related differences, e.g. due to the unlike partial and full core densities, frustrating any *a priori* estimate of their contribution to the potential energy correction δE_{V}. Nevertheless as the genuine differences are small and confined to the immediate vicinity of ion sites they should be rather inconsequential to the calculation of total energy differences. Such a scenario is conceivable and consistent with our results for Na, Al, Si, etc., but has its limitations as major portions of the valence charge density reside and adjust to charge transfer close to the ion sites. This clearly applies for the $2p$ states of the first row elements like C and the $3d$ transition metals like Cu, which take on their maxima in the domain of the genuine differences. Hence we find the potential energy correction for these elements to be only partly conditioned by the treatment of nonlinear CV XC. In case of Cu the $3d$ electrons are considered as valence rather than as core electrons so that their XC interactions with the $4s$ electrons are accounted for exactly and not linearly through pseudopotentials. For such a core-valence partitioning it is readily verified by inspection, *cf.* Fig. 2, that the differences of LDA and GGA pseudopotentials are primarily of the genuine kind and thus quite independent of a further account of nonlinear CV XC with still deeper core states. Accordingly we obtain an actually equivalent description of the bulk lattice parameters in GGA with either LDA or GGA pseudopotentials, with the potential energy correction to the cohesive en-

ergy being of the order of 0.2 eV within both linear and nonlinear CV XC. We would like to point to an analogous observation made in an all-electron method using pseudopotentials, where the full core density is retained: investigating Fe within the PW GGA, Cho *et al.*[24] reported nearly identical structural and magnetic parameters with either LDA or GGA based pseudopotentials.

V. SUMMARY AND CONCLUSIONS

In conclusion we have shown that GGA pseudopotentials indeed convey a substantial share of the GGA's corrections over LDA. Accordingly we deem the consistent use of the GGA in the application of the pseudopotential *and* their construction to be generally a key requirement to attain GGA quantities equivalent to those obtained within GGA all-electron methods. By contrast, inequivalent results arise when the XC energy is treated in GGA but the pseudopotentials are taken, inconsistently, to be the same ones as in LDA. We have found such "portability errors" to be most significant when the XC interaction of core and electrons is treated linearly as a component of the pseudopotential, but less important when the nonlinear core-valence XC interaction is incorporated properly into the XC energy functional of the valence electrons itself employing a partial core density. The precise agreement of the results for the cohesive energies from our perturbative and self-consistent calculations conforms with the the common lore[15,48] that self-consistency has only a small effect on the value of GGA total energies and differences thereof. Instead these can be accurately evaluated with the LDA wavefunctions and charge density. Our analysis shows however that such an *a posteriori* GGA scheme within the pseudopotential framework must treat the difference in the valence-valence XC energies and the ionic pseudopotentials on an equal footing, as given in Eq. (4): either carrying out the initial LDA calculation with LDA pseudopotentials and adding to the total energy the correction $\delta E_{\rm XC} + \delta E_{\rm V}$ or, equivalently, doing the LDA calculation with GGA pseudopotentials ($\delta E_{\rm V} \equiv 0$) and adding just $\delta E_{\rm XC}$ to the total energy.

As the differences of the pseudopotentials originate from the distinct core-valence XC potentials in LDA and GGA we moreover understand our findings as evidence that the bond softening in GGA is directly related to a stronger XC repulsion between the valence and upper core states than in the LDA. The reduction of the binding energy by the GGA on the other hand appears to a larger extent due to describing the XC of the valence electrons among themselves within GGA instead of LDA. The notion of a more repulsive nature of GGA core-valence XC agrees with and qualifies earlier observations that the GGA corrections to bonding properties in solids arise mainly from the immediate vicinity of the ions rather than from the interstitial regions.[57] Likewise it is supported by the fact that the GGA XC potential of atoms like the exact XC potential is superimposed with a peaked structure which acts repulsively at shell boundaries compared to the LDA XC potential.[30] Interestingly our findings suggest that inadequacies in the description of core-valence XC are an important aspect of deficiencies in the description of chemical bonds within either LDA or GGA.

In concluding we note that a conceptual parallel of the ("inconsistent") combination of LDA pseudopotentials with GGA XC is encountered in wavefunction-based many-body methods such as quantum Monte-Carlo (QMC) simulations.[58] In applications QMC has been mostly combined with pseudopotentials derived from effective one-particle schemes.[59] Thereby the interactions among the valence electrons are described exactly whereas the effects of the core electrons are dealt with in an approximate manner, say, on the level of LDA. In principle such QMC calculations provide an exact reference against which we could check the performance of approximate XC schemes like the GGA for the valence electrons alone. Indeed a survey of the literature indicates that cohesive energies for diamond, Si,[60,61] and Ge[62] obtained with QMC and LDA pseudopotentials are in significantly closer agreement with experimental figures than are our GGA results using LDA pseudopotentials. At least for these cases this raises the question whether the GGA affords a better description of XC among *all* electrons, then yielding highly accurate binding energies, than of XC among the valence electrons alone. On the other hand, one is well aware that the use of LDA pseudopotentials in QMC simulations introduces some uncertainty in the QMC values for the cohesive energy themselves,[59,62] quite analogous to the "portability errors" we have found in GGA calculations using LDA pseudopotentials to be of the order of up to some tenths of an eV. On this level of accuracy it is then clearly desirable to obtain accurate estimates of the systematic uncertainties related to the use of pseudopotentials derived from DFT in exact methods like e.g. QMC simulations as well in order to facilitate a quantitative assessment of approximate XC schemes like the GGA.

VI. APPENDIX

In this appendix we present some tests on the transferability of our GGA pseudopotentials compared to the LDA ones. These serve to further corroborate that GGA and LDA pseudopotentials show a similar inherent transferability but exhibit significant differences due to core-valence (CV) XC, as discussed in Sec. II. As is rather well established transferable pseudopotentials should closely preserve: (1) The all-electron atomic scattering properties as given by the logarithmic derivatives at some radius outside the core region over the range of valence energies relevant to chemical bonding, say up to ± 1 hartree about the reference energies. (2) The all-electron atomic hardness,[63,64] i.e. reproduce total energy and eigenvalues for excited atomic configurations, to within the accuracy of the the underlying frozen-core approximation.

In Fig. 4 we show the logarithmic derivatives evaluated with screened pseudopotentials, *cf.* Eq. (5), taking germanium as an example. Good agreement with the respective all-electron logarithmic derivatives, to be expected from the norm-conservation constraints, is con-

firmed for both LDA as well as GGA pseudopotentials in the semilocal and also in the Kleinman-Bylander representation. For the latter we have additionally verified the absence of ghost states following Gonze *et al.*[65]

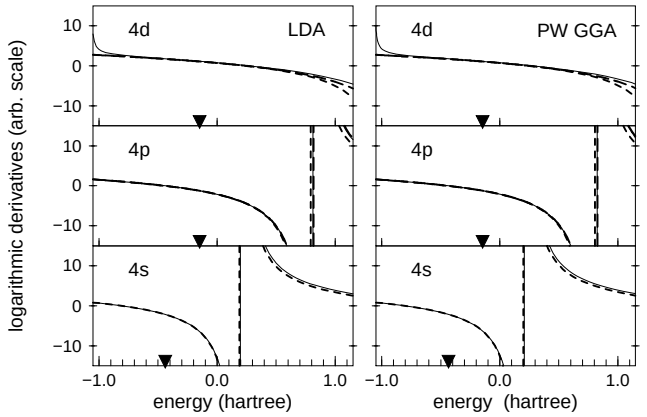

FIG. 4. Logarithmic derivatives $R_l'(\varepsilon)/R_l(\varepsilon)$ vs. energy ε for the germanium atom (at $r = 2.4$ bohr, and with the $4s$-component as local potential). Solid lines correspond to the all-electron potential, dashed lines to the semilocal pseudopotentials, and long-dashed lines to their Kleinman-Bylander form. Reference energies are marked by solid triangles. In the all-electron case the pole in the $4d$-channel at ≈ -1 hartree is associated with the $3d$ core state.

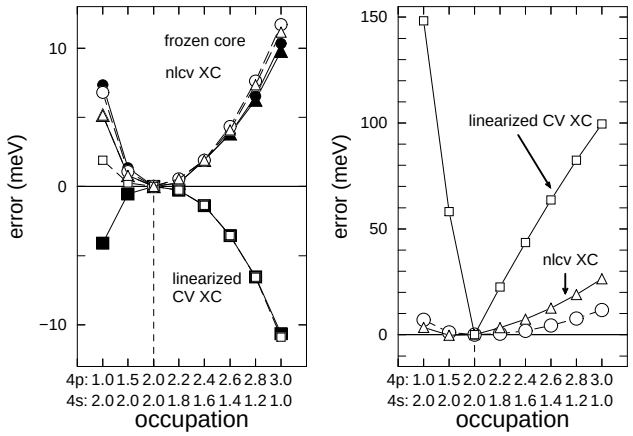

FIG. 5. Deviations in the excitation energies of the germanium pseudo atom compared to all-electron results, calculated from total energy differences with respect to the groundstate configuration. The left panel corresponds to the consistent approach using the same XC scheme throughout. The right panel refers to the inconsistent approach, using the LDA pseudopotential but GGA for the XC energy. Solid symbols stand for LDA, open symbols for PW GGA values. Squares (□) correspond to calculations within linearized CV XC, and triangles (△) to those within nonlinear CV XC. Results obtained within the frozen-core approximation are shown for comparison and marked by circles (○). Lines are meant to guide to the eyes. Note that the underlying excitation energies reach up to ≈ 8 eV.

We have applied criterion (2) employing excited neutral and (positively) ionized configuations of the spherical isolated atom. In the case of Ge, e.g., examining a $4s \rightarrow 4p$ electron transfer to mimic orbital hybridization upon bond formation, and the first ionization potential. In Fig. 5 we plot the error of the excitation energies for consistent calculations within LDA and GGA with respect to all-electron calculations.

For linearized CV XC we find the ensuing errors to be of the same magnitude albeit of opposite sign as those in a frozen-core calculation, where only the all-electron valence states are allowed to adjust self-consistently but the core charge density is kept fixed as that in the atomic groundstate. For nonlinear CV XC the errors of the pseudopotential calculation approach those of the frozen-core calculation. Thus we conclude that the pseudopotential related errors are indeed comparably small, absolutely and relatively, as those due to neglect of core relaxation, the excitation energy for the transfer $(4s^2, 4p^2) \rightarrow (4s^1, 4p^3)$ being about 8 eV. Carrying out the tests in inconsistent manner – using GGA XC and LDA pseudopotentials with linearized CV XC – leads to large devations.

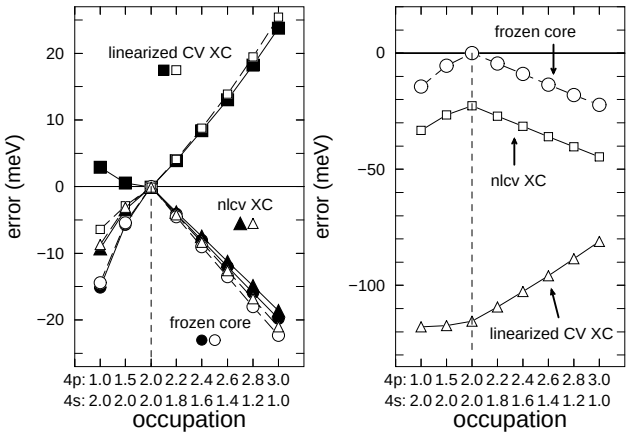

FIG. 6. Deviations of the level spacing of the $4s$ and $4p$ states of the germanium atom with respect to all-electron results. See Fig. 5 for a legend. The level spacing is ≈ 8 eV for the groundstate configuration, and varies by ≈ 0.8 eV.

Particularly excitation energies are overestimated compared to full GGA calculations, suggesting that the pseudopotentials in LDA are more attractive than in GGA, in accordance with our findings in Sec. II and IV. Employing LDA pseudopotentials together with nonlinear CV XC we obtain agreement with the GGA frozen-core calculation however. Considering the eigenvalues we have observed an analogous pattern. This is illustrated in Fig. 6 for the deviation of the level spacing $\varepsilon 4p - \varepsilon 4s$ with respect to all-electron calculations within LDA and GGA. Again a large error occurs in case of the inconsistent GGA calulation using LDA pseudopotentials and linearized CV XC, while the consistent approach is accurate, errors being of the order of a few ten meV compared to changes in the level spacing of about 0.8 eV.

In summary these tests affirm our conclusion reached for the bulk systems: Within GGA and LDA the respective pseudopotentials possess similar transferability, errors due to the usual linearization of CV XC being small; LDA pseudopotentials are adequate in GGA calculations (and vice versa) only if CV XC, acting more repulsively in GGA compared to LDA, is incorporated explicitly.

* Present address: Lehrstuhl für Theoretische Festkörperphysik, Universität Erlangen, Staudtstrasse 7/B2, D-91058 Erlangen, Germany.
† Present address: Physik Department T30, Universität München, James-Franck-Strasse, D-85747 Garching, Germany.

[1] D. C. Langreth, M. J. Mehl, Phys. Rev. Lett. **47**, 446 (1981); Phys. Rev. B **28**, 1809 (1983).
[2] J. P. Perdew, Phys. Rev. Lett. **55**, 1665 (1985).
[3] A. D. Becke, Phys. Rev. A **38**, 3098 (1988).
[4] J. P. Perdew, Phys. Rev. B **33**, 8822 (1986); J. P. Perdew, Phys. Rev. B **34**, 7406 (1986).
[5] J. P. Perdew, J. A. Chevary, S. H. Vosko, K. A. Jackson, M. R. Pederson, D. J. Singh, C. Fiolhais, Phys. Rev. B **46**, 6671 (1992).
[6] P. Hohenberg, W. Kohn, Phys. Rev. **136**, B 864 (1964).
[7] R. M. Dreizler, E. K. U. Gross, *Density Functional Theory* (Springer Verlag, Berlin, 1990).
[8] W. Kohn, L. Sham, Phys. Rev. **140**, A1133 (1965).
[9] R. O. Jones, O. Gunnarsson, Rev. Mod. Phys. **61**, 689 (1989).
[10] B. G. Johnson, P. M. W. Gill, J. A. Pople, J. Chem. Phys. **98**, 5612 (1993).
[11] A. D. Becke, J. Chem. Phys. **97**, 9173 (1992).
[12] P. H. T. Philipsen, E. J. Baerends, Phys. Rev. B **54**, 5326 (1996).
[13] M. Körling, J. Häglund, Phys. Rev. B **45**, 13293 (1992).
[14] A. Garcia, C. Elsässer, J. Zhu, S. G. Louie, Phys. Rev. B **46**, 9829 (1992); Phys. Rev. B **47**, 4150 (1993).
[15] B. Hammer, J. K. Nørskov, Phys. Rev. Lett. **73**, 3971 (1993).
[16] B. Hammer, M. Scheffler, K. W. Jacobsen, J. K. Nørskov, Phys. Rev. B **73**, 1400 (1994).
[17] E. Pehlke, M. Scheffler, Phys. Rev. Lett. **74**, 952 (1995).
[18] D. Porezag, M. R. Pederson, J. Chem. Phys. **102**, 9345 (1995).
[19] J. Baker, M. Muir, J. Andzelm, J. Chem. Phys. **102**, 2063 (1995).
[20] L. Fan, T. Ziegler, J. Am. Chem. Soc. **114**, 10890 (1992).
[21] T. C. Leung, C. T. Chan, B. N. Harmon, Phys. Rev. B **44**, 2923 (1991).
[22] D. R. Hamann, Phys. Rev. Lett. **76**, 660 (1996).
[23] N. Moll, M. Bockstedte, M. Fuchs, E. Pehlke, M. Scheffler, Phys. Rev. B **52**, 2550 (1995).
[24] J.-H. Cho, M. Scheffler, Phys. Rev. B **53**, 10685 (1996).
[25] A. Khein, D. J. Singh, C. J. Umrigar, Phys. Rev. B **51**, 4105 (1995).
[26] V. Ozoliņš, M. Körling, Phys. Rev. B **48**, 18304 (1993).
[27] A. Dal Corso, A. Pasquarello, A. Baldereschi, R. Car, Phys. Rev. B **53**, 1180 (1996).
[28] C. Filippi, D. J. Singh, C. J. Umrigar, Phys. Rev. B **50**, 14947 (1994).
[29] G. Ortiz, Phys. Rev. B **45**, 11328 (1992).
[30] C. J. Umrigar, X. Gonze, in *Proceedings of the Mardi Gras 1993 Conference*, D. A. Browne *et al.*, eds. (World Scientific, Singapore, 1993), p. 43; C. J. Umrigar, X. Gonze, Phys. Rev. A **50**, 3827 (1994).
[31] A. Zupan, J. P. Perdew, K. Burke, M. Causa, Intl. Journ. Quantum Chem. **61**, 835 (1997).
[32] W. E. Pickett, Comput. Phys. Rep. **9**, 115 (1989).
[33] Y. -M. Juan, E. Kaxiras, Phys. Rev. B **48**, 14944 (1993).
[34] Y. -M. Juan, E. Kaxiras, R. G. Gordon, Phys. Rev. B **51**, 9521 (1995).
[35] P. Nachtigall, K. J. Jordan, A. Smith, H. Jóhnsson, J. Chem. Phys. **104**, 148 (1996).
[36] B. Hammer, Y. Morikawa, J. K. Nørskov, Phys. Rev. Lett. **76**, 2141 (1996).
[37] P. Kratzer, B. Hammer, J. K. Nørskov, J. Chem. Phys. **105**, 5595 (1996).
[38] A. Becke, J. Chem. Phys. **104**, 1040 (1996).
[39] J. P. Perdew, K. Burke, M. Ernzerhof, Phys. Rev. Lett. **77**, 3865 (1996).
[40] M. Fuchs (unpublished).
[41] U. von Barth, C. D. Gelatt, Phys. Rev. B **21**, 2222 (1980).
[42] J. Ihm, A. Zunger, M. L. Cohen, J. Phys. C **12**, 4409 (1979).
[43] D. R. Hamann, M. Schlüter, C. Chiang, Phys. Rev. Lett. **3**, 1494 (1979).
[44] N. Troullier, J. L. Martins, Phys. Rev. B **43**, 1993 (1991).
[45] G. B. Bachelet, D. R. Hamann, M. Schlüter, Phys. Rev. B **26**, 4199 (1982).
[46] J. Hebenstreit, M. Scheffler, Phys. Rev. B **46**, 10134 (1992).
[47] S. G. Louie, S. Froyen, M. L. Cohen, Phys. Rev. B **26**, 1738 (1982).
[48] X. J. Kong, C. T. Chan, K. M. Ho, Y. Y. Ye, Phys. Rev. B **42**, 9357 (1990).
[49] M. Fuchs, M. Scheffler, Comput. Phys. Commun. (in preparation).
[50] L. Kleinman, D. M. Bylander, Phys. Rev. Lett. **48**, 1425 (1982).
[51] We employed the `fhi93cp` plane wave total energy code [R. Stumpf, M. Scheffler, Comput. Phys. Commun. **79**, 447 (1994); M. Bockstedte, A. Kley, J. Neugebauer, M. Scheffler, *ibid.* (to be published)], in a version extended to GGAs.
[52] F. D. Murnaghan, Proc. Natl. Acad. Sci. USA **30** , 244 (1944).
[53] This estimate was obtained by the Debye model taking Debye temperatures from [J. de Launay, *Solid State Physics*, F. Seitz, D. Turnbull, eds. (Academic Press, New York, 1956)].
[54] H. J. Monkhorst, J. D. Pack, Phys. Rev. B **13**, 5188 (1976).
[55] Repeating our calculations for Al, Si, and Ge with Hamann type pseudopotentials [D. R. Hamann, Phys. Rev. B **40**, 2980 (1989)], we have not found significant changes in the differences between the LDA and GGA results. Within either XC scheme changes amounted to $\lesssim$1% for lattice constants, $\lesssim$3% for the bulk moduli, and $\lesssim$0.1 eV for the binding energies.
[56] F. W. Kutzler, G. S. Painter, Phys. Rev. Lett. **59**, 1285 (1987).
[57] G. Kresse, J. Furthmüller, J. Hafner, Phys. Rev. B **50**, 13181 (1994).
[58] see, e.g., L. Mitáš, Comput. Phys. Commun. **96**, 107 (1996).
[59] E. L. Shirley, R. M. Martin, G. B. Bachelet, D. M. Ceperley, Phys. Rev. B **42**, 5057 (1990).
[60] S. Fahy, X. W. Wang, S. G. Louie, Phys. Rev. B **42**, 3503 (1990).
[61] X. -P. Li, D. M. Ceperley, R. M. Martin, Phys. Rev. B **44**, 10929 (1991).
[62] G. Rajagopal, R. J. Needs, A. James, S. D. Kenny, W. M. C. Foulkes, Phys. Rev. B **51**, 10591 (1995).
[63] M. Teter, Phys. Rev. B **48**, 5031 (1993).
[64] A. Filippetti, D. Vanderbilt, W. Zhong, Y. Cai,

G. B. Bachelet, Phys. Rev. B **52**, 11793 (1995).
[65] X. Gonze, R. Stumpf, M. Scheffler, Phys. Rev. B **44**, 8503 (1991).
[66] Experimental lattice constants are taken from *Semiconductors, Group IV Elements and III-V Compounds*, edited by O. Madelung, (Springer-Verlag, Berlin, 1991), and *Landolt-Börnstein*, New Series, Group III, Vols. 6 and 7, edited by K.-H. Hellwege and A. M. Hellwege (Springer-Verlag, Berlin, 1971). Bulk moduli are based on the elastic constant data in *Landolt-Börnstein*, New Series, Group III, Vols. 1 and 2, edited by K.-H. Hellwege and A. M. Hellwege (Springer-Verlag, Berlin, 1969). Cohesive energies are quoted from C. Kittel, *Introduction to Solid State Physics* (Wiley, New York, 1986), and W. A. Harrison, *Electronic Structure and the Properties of Solids* (Dover Publications, New York, 1989).

TABLE I. Cohesive properties of Na. The first column indicates the XC scheme used to generate the pseudopotentials, the second the one employed for the XC energy of the (pseudo) atom and solid. Bracketed values are based on nonlinear core-valence XC. We show the lattice constant a_0, the bulk modulus B_0, and the cohesive energy E_b. The latter includes a spin correction of the free Na atom of 0.20 eV (LDA) and 0.22 eV (GGA).

potential	$E_{\rm XC}$	a_0 (Å)	B_0 (GPa)	E_b (eV)
LDA	LDA	3.98 (4.05)	8.7 (9.1)	1.28 (1.22)
LDA	BP	3.97 (4.22)	8.7 (7.3)	1.06 (0.94)
BP	BP	4.20 (4.22)	7.3 (7.4)	0.94 (0.94)
LDA	PW	3.98 (4.21)	8.7 (7.3)	1.19 (1.08)
PW	PW	4.24 (4.21)	7.0 (7.3)	1.05 (1.08)
LDA[a]		4.05	9.2	
PW[a]		4.22	7.1	
Experiment[b]		4.23	6.92	1.11

[a]All-electron data from Reference 5.
[b]Reference 66.

TABLE II. Cohesive properties of NaCl. Like Table I, and using a spin correction of 0.20 eV (LDA) and 0.22 eV (GGA) for the free Cl atom.

potential	$E_{\rm XC}$	a_0 (Å)	B_0 (GPa)	E_b (eV)
LDA	LDA	5.19 (5.43)	32 (32)	7.28 (6.99)
LDA	BP	5.27 (5.67)	27 (22)	6.59 (6.24)
BP	BP	5.74 (5.68)	21 (22)	6.20 (6.19)
LDA	PW	5.28 (5.65)	28 (23)	6.85 (6.43)
PW	PW	5.87 (5.66)	18 (23)	6.22 (6.40)
Experiment[a]		5.64	24.5	6.51

[a]Reference 66.

TABLE III. Cohesive properties of hcp Mg. Like Table I. The equilibrium c/a ratio was obtained as 1.59 (LDA) and 1.66 (GGA), the experimental value is 1.62.[a]

potential	$E_{\rm XC}$	a_0 (Å)	B_0 (GPa)	E_b (eV)
LDA	LDA	3.05 (3.16)	39 (37)	2.09 (1.76)
BP	BP	3.17 (3.18)	32 (31)	1.27 (1.22)
PW	PW	3.20 (3.20)	30 (32)	1.42 (1.40)
Experiment[a]		3.21	35.4	1.51

[a]Reference 66.

TABLE IV. Cohesive properties of Al. Like Table I, including a spin correction of the free Al atom of 0.15 eV (LDA) and 0.19 eV (GGA).

potential	$E_{\rm XC}$	a_0 (Å)	B_0 (GPa)	E_b (eV)
LDA	LDA	3.97 (3.97)	83 (85)	4.09 (4.09)
LDA	BP	3.97 (4.03)	80 (75)	3.39 (3.27)
BP	BP	4.05 (4.05)	75 (75)	3.26 (3.25)
LDA	PW	3.97 (4.02)	81 (77)	3.64 (3.54)
PW	PW	4.05 (4.04)	79 (79)	3.52 (3.53)
LDA[a]		3.98	83.9	
PW[a]		4.10	72.6	
Experiment[b]		4.05	77.3	3.39

[a]All-electron data from Reference 25.
[b]Reference 66.

TABLE V. Cohesive properties of diamond. Like Table I, using a spin correction of 1.13 eV (LDA) and 1.26 eV (GGA) for the C atom.

potential	$E_{\rm XC}$	a_0 (Å)	B_0 (GPa)	E_b (eV)
LDA	LDA	3.54 (3.54)	436 (436)	8.96 (8.93)
LDA	BP	3.55 (3.58)	421 (406)	7.93 (7.57)
BP	BP	3.59 (3.59)	399 (400)	7.56 (7.58)
LDA	PW	3.54 (3.58)	424 (406)	8.09 (7.92)
PW	PW	3.58 (3.58)	408 (405)	7.80 (7.83)
Experiment[a]		3.57	442	7.37

[a]Reference 66.

TABLE VI. Cohesive properties of Si. Like Table I, using a spin correction of 0.66 eV (LDA) and 0.79 eV (GGA) for the Si atom.

potential	$E_{\rm XC}$	a_0 (Å)	B_0 (GPa)	E_b (eV)
LDA	LDA	5.38 (5.39)	94 (94)	5.34 (5.32)
LDA	BP	5.40 (5.46)	91 (86)	4.60 (4.47)
BP	BP	5.47 (5.47)	85 (85)	4.46 (4.45)
LDA	PW	5.39 (5.45)	92 (87)	4.79 (4.66)
PW	PW	5.46 (5.46)	87 (87)	4.64 (4.64)
LDA[a]		5.41	96	5.28
BP[a]		5.54	80	
PW[a]		5.50	83	
Experiment[b]		5.43	98.8	4.63

[a]All-electron data from Reference 28.
[b]Reference 66.

TABLE VII. Cohesive properties of Ge. Like Table I, using a spin correction of 0.60 eV (LDA) and 0.74 eV (GGA) for the Ge atom

potential	$E_{\rm XC}$	a_0 (Å)	B_0 (GPa)	E_b (eV)
LDA	LDA	5.56 (5.60)	73 (71)	4.75 (4.58)
LDA	BP	5.59 (5.74)	67 (57)	3.96 (3.66)
BP	BP	5.73 (5.76)	59 (56)	3.70 (3.66)
LDA	PW	5.58 (5.74)	69 (59)	4.14 (3.82)
PW	PW	5.74 (5.74)	58 (58)	3.82 (3.82)
LDA[a]		5.63	78	4.54
BP[a]		5.76	60	
PW[a]		5.75	61	
Experiment[b]		5.66	76.8	3.85

[a]All-electron data from Reference 28.
[b]Reference 66.

TABLE VIII. Cohesive properties of GaAs. Like Table I, using a spin correction of 0.15 eV (LDA) and 0.18 eV (GGA) for the Ga, and 1.41 eV (LDA) and 1.67 eV (GGA) for the As atom.

potential	$E_{\rm XC}$	a_0 (Å)	B_0 (GPa)	E_b (eV)
LDA	LDA	5.50 (5.57)	79 (75)	8.68 (8.15)
LDA	BP	5.52 (5.72)	74 (62)	7.19 (6.33)
BP	BP	5.68 (5.72)	64 (62)	6.52 (6.33)
LDA	PW	5.51 (5.70)	76 (64)	7.51 (6.63)
PW	PW	5.69 (5.71)	63 (64)	6.74 (6.63)
LDA[a]		5.62	74	7.99
BP[a]		5.76	60	
PW[a]		5.74	65	
Experiment[b]		5.65	74.8	6.52

[a]All-electron data from Reference 28.
[b]Reference 66.

TABLE IX. Cohesive properties of fcc Cu. Like Table I, using a spin correction of 0.20 eV (LDA) and 0.25 eV (GGA).

potential	$E_{\rm XC}$	a_0 (Å)	B_0 (GPa)	E_b (eV)
LDA	LDA	3.55 (3.56)	172 (172)	4.31 (4.24)
LDA	BP	3.68 (3.70)	124 (122)	3.09 (3.06)
BP	BP	3.67 (3.68)	130 (131)	3.22 (3.23)
LDA	PW	3.67 (3.69)	127 (123)	3.23 (3.20)
PW	PW	3.67 (3.67)	134 (132)	3.38 (3.38)
LDA[a]		3.52	192	4.29
BP[a]		3.62	151	3.12
PW[a]		3.62	151	3.30
Experiment[b]		3.60	138	3.50

[a] All-electron values from Ref. 25 (a_0, B_0), and Ref. 12 (E_b).
[b]Reference 66.

TABLE X. Cohesive properties of bcc W. Like Table I, using a spin correction of 2.04 eV (LDA) and 2.32 eV (GGA).

potential	$E_{\rm XC}$	a_0 (Å)	B_0 (GPa)	E_b (eV)
LDA	LDA	3.14 (3.16)	324 (331)	10.76 (10.24)
LDA	BP	3.15 (3.21)	308 (306)	9.26 (8.52)
BP	BP	3.20 (3.21)	299 (308)	8.73 (8.54)
LDA	PW	3.14 (3.20)	313 (308)	9.63 (8.87)
PW	PW	3.22 (3.21)	298 (310)	8.88 (8.87)
LDA[a]		3.14	337	
PW[a]		3.19	307	
Experiment[b]		3.16	310	8.90

[a]All-electron values from Ref. 25.
[b]Reference 66.

TABLE XI. Change of the cohesive energy, δE_b, due to the replacem
energy change per atom as obtained from self-consistent calculations, δE
The latter is decomposed into its consituent terms arising from the d
pseudopotentials, $\delta E_{\rm V}$. The values without and with brackets correspond
nonlinear core-valence XC respectively. No spin-corrections were applied t
at their experimental values in all calculations, the ensuing error of the t
equilibrium structure staying below ≈50 meV per atom. Symbols are exp

		$\delta E_{\rm tot}^{\rm solid}$ (eV)
Na	$\delta E_{\rm tot}$	0.32 (-3.21)
	$\delta E_{\rm XC} + \delta E_{\rm V}$	0.32 (-3.20)
	$\delta E_{\rm XC}$	-0.01 (-3.20)
	$\delta E_{\rm V}$	0.33 (-0.00)
Diamond	$\delta E_{\rm tot}$	0.31 (-1.42)
	$\delta E_{\rm XC} + \delta E_{\rm V}$	0.32 (-1.40)
	$\delta E_{\rm XC}$	-0.46 (-1.37)
	$\delta E_{\rm V}$	0.78 (-0.03)
Si	$\delta E_{\rm tot}$	0.60 (-0.97)
	$\delta E_{\rm XC} + \delta E_{\rm V}$	0.61 (-0.96)
	$\delta E_{\rm XC}$	-0.27 (-1.09)
	$\delta E_{\rm V}$	0.88 (0.13)
Ge	$\delta E_{\rm tot}$	1.50 (-5.50)
	$\delta E_{\rm XC} + \delta E_{\rm V}$	1.50 (-5.48)
	$\delta E_{\rm XC}$	-0.24 (-5.49)
	$\delta E_{\rm V}$	1.74 (0.01)
Cu	$\delta E_{\rm tot}$	1.63 (-1.99)
	$\delta E_{\rm XC} + \delta E_{\rm V}$	1.64 (-1.99)
	$\delta E_{\rm XC}$	-5.54 (-7.48)
	$\delta E_{\rm V}$	7.19 (5.50)